

Interfacial Modification Boosted Permittivity and Triboelectric Performance of Liquid Doping Composites for High-performance Flexible Triboelectric Nanogenerators

Titao Jing, Bingang Xu*, Yujue Yang, Chenghanzhi Jiang, Mengjie Wu

Nanotechnology Center, Institute of Textiles and Clothing, The Hong Kong

Polytechnic University, Hung Hom, Kowloon 999077, Hong Kong

* Corresponding author, E-mail: texubg@polyu.edu.hk

Abstract:

Composites' interface is the contact area between filler and matrix, which is a critical issue in composites' permittivity and thereby of great value to improve friction composites' performance in triboelectric nanogenerators (TENGs). However, composites' interfacial influence on triboelectric performance was not clear in past years even numerous composites were prepared, which limited materials' advance of triboelectric performance. Here, a systematic investigation about the composites' interfacial influence was performed on liquid doping polydimethylsiloxane (PDMS) composites, in which interfacial area and compatibility were found with great importance to composites' permittivity and triboelectric performance. Through high preparation stirring speed and appropriate surfactant additive, interfacial modification of enlarging interfacial area and compatible interface was facilely achieved. The as-prepared composites' permittivity and triboelectric performance were remarkably promoted as compared to composites without interfacial modification, achieving 8.1-

fold in output voltage and 9.5-fold in output current of pristine PDMS. Further, the composites were applied to assemble TENG for energy harvesting and movement detection. This work revealed the interface properties' influence on composites permittivity and further demonstrated the importance of interfacial modification for enhancement of triboelectric performance, illustrating that the interface issues should be taken into consideration in doping triboelectric composites for high output performance TENG.

Key words: Interfacial modification; Liquid doping composites; High permittivity composites; Polydimethylsiloxane; Triboelectric materials

1. Introduction

With the advent of mobile and next-generation portable electronics for applications in communication, personal health care, and environmental monitoring, the energy supplement of such devices emerged as an urgent issue.[1-5] Triboelectric nanogenerator (TENG), a device of electricity generator by converting mechanical energy, was widely accepted as a promising energy source to alleviate the aforementioned issue as the merits of low weight, ease of manufacturing, and high efficiency, which was first invented by Wang research group in 2012.[6, 7] TENGs were composed of two separated materials with back electrodes, which possessed different electron affinities and were termed as electronegative and electropositive materials.[8-13] Generally, triboelectric materials were critical to TENGs' energy density as the

triboelectricity were decided by the friction of materials and tremendous efforts had been committed to the development of materials with high output performance for various types TENG devices.[14, 15]

According to theory study of TENG device, triboelectric materials are not only friction materials but also the materials to store charge from friction.[8, 16, 17] Consequently, the improvement in friction materials' capacitance will bring into high output performance of TENG device.[17] Therefore, much effort had been made to improve the friction composites' permittivity through doping method on the basis of pristine triboelectric materials and the strategy had been proved its value in high output performance TENG.[15, 17-20] However, it should be emphasized that a large amount of interfacial areas were created in composites when fillers were introduced to friction matrix. The interface is the contact area between filler and matrix, which plays a critical role in composites permittivity as it decides the polarization, breakdown strength and defects of composites.[21, 22] Interfacial modification, including appropriate binding between two distinct fillers and matrix as well as large interfacial area, was thereby put forward in polymer matrix based composites for improvement of composites' permittivity, as it is crucial to improve the interfacial polarization with decreasing negative effects and consequently affording a high energy density or permittivity.[21, 23-25] Unfortunately, although numerous fillers had been employed in triboelectric composites to date, the influence of interface between fillers and matrix on composites' permittivity as well as triboelectric performance was lack of study and not clear, which limited triboelectric materials' advance in power density. Traditionally, the doping

materials used in triboelectric composites were usually solids, which were hard to disperse in pristine triboelectric materials due to their giant interface difference.[17, 19, 26-28] In addition, the interfacial modification in solid doping materials usually relied on chemical process to couple with organic group such as siloxane on solid surface.[21-23] The process might be difficult as the solid surface is usually short of reactive group for coupling. The complex process thus limited the study of interface's influence on materials triboelectric performance even it is of great value in TENG's output performance.

In our previous work, high permittivity liquid, instead of commonly solid materials, was introduced to polydimethylsiloxane as doping materials for high output performance TENG. [29] That was high permittivity liquid doping PDMS (PDMS-HD). The critical preparation process of liquid doping composites employed PDMS pre-cured liquid state to form the precursor emulsion mixture, in which the liquid was dispersed in PDMS pre-cured liquid as micro-droplets. Via heat assistant curing of PDMS pre-cured liquid, PDMS matrix was formed and the micro-droplets were consequently encapsulated in PDMS matrix. The introduced high permittivity liquid increased the permittivity of composite as well as reduced the effective thickness of pristine friction materials, which enhanced the capacitance of friction materials as well as triboelectric performance of corresponding TENG.[16, 17, 30] Compared to solid doping materials, liquid is deformable and can be easily changed its interface. For instance, shearing force of liquid generated by flow velocity could tailor the size of emulsion's dispersed droplets which are correlated to the interfacial area.[31-34] Hence,

the deformable liquid doping materials are suitable to study the interfacial area's influence on composites permittivity as well as triboelectric performance by simply adjusting its flow velocity in precursor emulsion mixture. More importantly, the liquid could be applied as functional molecules micro-carrier to fabricate functionalization materials, which avoided chemical reaction and indicated a promising method of functionalization.[29] The numerous surfactants thus could be applied to tailor the interfacial compatibility of liquid doping materials without chemical reaction, which provided various and powerful choices.

Herein, we put a systematic investigation about the influence of dispersed liquid droplets' interface on composite's permittivity and exploited it to maximize the triboelectric performance of composite. Via vigorous stirring and surfactant assistance, the interface between high permittivity liquid droplets and PDMS matrix was remarkably improved, which further resulted in the increase of composites' permittivity. The triboelectric performance of composite thus could be improved to as much as 8.1 folds in output voltage and 9.5 folds in output current as compared to pristine PDMS. This work presented the relationship between interface properties and composites' permittivity and further demonstrated the great value of interfacial modification in triboelectric performance enhancement. The conclusion in this work illustrated that the interface issues should be taken into consideration in doping triboelectric composites, which would promote the advancement in high output performance triboelectric materials.

2. Results and discussion

2.1 Relationship of interface, capacitance and triboelectric performance of doping triboelectric materials.

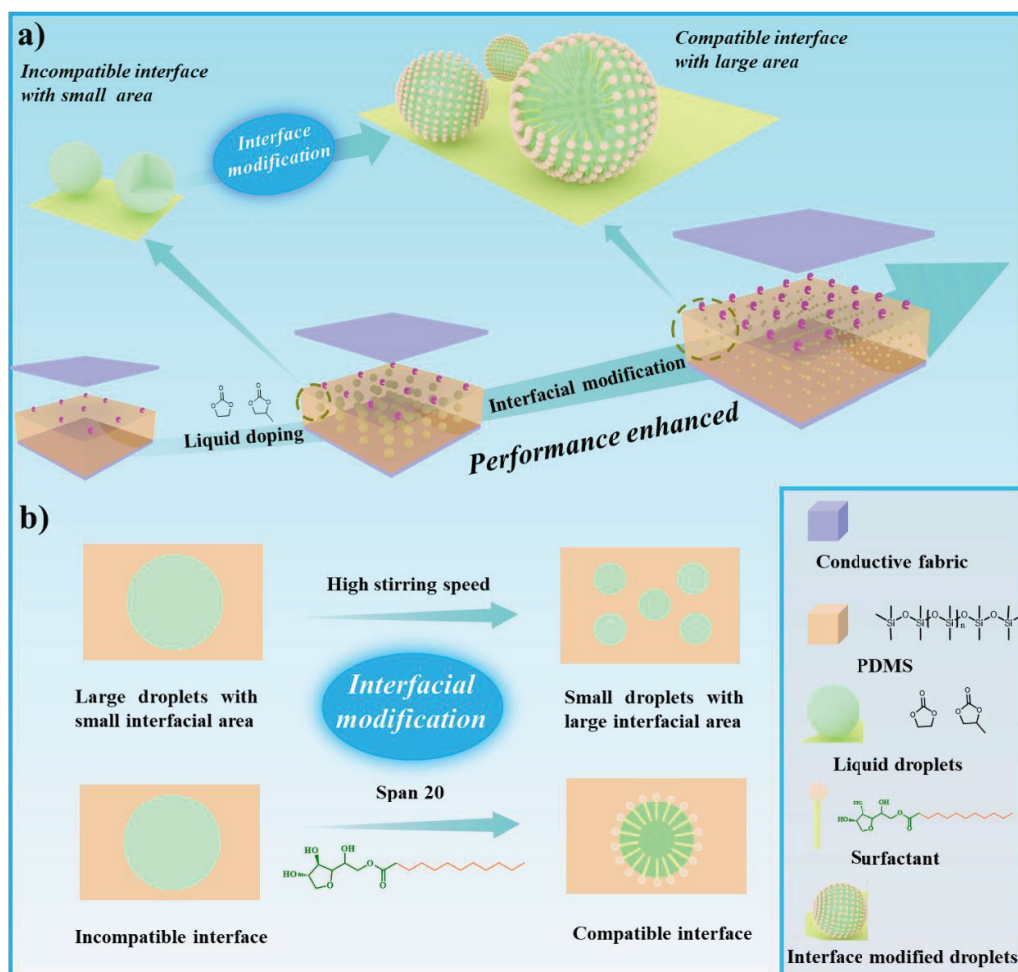


Figure 1. Scheme of interface modified liquid doping PDMS composite. a) Stepwise increases the output performance by interface modified high permittivity liquid doping PDMS. b) High stirring speed to prepare small liquid droplets, which increase interfacial area. Span 20 was introduced in liquid doping PDMS to increase the interfacial compatibility between doping liquid and PDMS.

The TENG working mode could be divided into four types in which vertical contact-separation mode is the most common mode. In a typical vertical contact-separation mode TENG, TENG is composed of two paired friction materials with corresponding back electrode. By some excellent theoretical studies of vertical contact-

separation mode, the TENG is not only regarded as an energy generator but also a device to store energy.[16, 17] The principle points out that triboelectric charge density of TENG is critical in its output performance and its capacitance decides the capability of triboelectric charge. Consequently, improvement of capacitance of the TENG would boost TENG's output performance, which had been proved its value by many published works.[17, 19, 20] According to the theoretical research of TENG and capacitance, the capacitance could be described by following ideal equation

$$C_{max} = \varepsilon_0 * S \frac{\varepsilon_r}{d} \quad (1)$$

in which C_{max} is the capacitance of triboelectric materials, and the ε_r , d , S are permittivity, effective thickness and contact area of friction materials, respectively.[17] Furthermore, ε_r has a proportional correlation to the filling materials permittivity and its filling ratio when the triboelectric materials are doped to prepare composites.[23] The theoretical equation is

$$\varepsilon_r = \varepsilon_m * V_m + \varepsilon_f * V_f \quad (2)$$

ε_m and V_m are the permittivity and volumetric ratio of matrix; ε_f and V_f are the permittivity and volumetric ratio and filling materials.[30, 35] Therefore, the high permittivity materials that are introduced in friction materials in TENG will increase its capacitance and further promote its output performance.

Because of the great importance of triboelectric materials' capacitance in TENGs output performance, much effort had been made to improve the triboelectric composites' permittivity through doping method on the basis of pristine friction materials.[15, 17, 19] However, composite permittivity was decided by complex factors. Based on the

permittivity theory of filler in composite, not only matrix and filling materials' permittivity and their mixing ratios, but also the interface between matrix and filling materials also had directly great influence on composite's permittivity.[23, 30] The interfacial area between the matrix and particle was reversely proportional to the size of particle and large interfacial area would boost the exchange coupling effect through a dipolar interface layer, affording higher polarization levels, dielectric response, and breakdown strength.[23, 30] In addition, appropriate coupling agent between two distinct filler and matrix could boost the interface binding strength or compatibility, which was crucial to improve the interfacial polarization with decreasing negative effects and consequently affording a high energy density or permittivity.[22, 23] The composite permittivity as well as output performance thus would be promoted by such appropriately interfacial modification. As shown in Fig 1 and S1, the high permittivity liquid was dispersed as micro-droplets in the continuous phase of PDMS pre-cured solution and precursor liquid-liquid emulsion system was formed, in which the liquid-liquid interface between droplets and PDMS pre-cured solution was created. While the PDMS pre-cured solution was cured to form PDMS matrix, the high permittivity liquid was reserved in the composite consequently and liquid doping PDMS composites was formed. The reserved high permittivity liquid thus was applied as the filling materials to improve the permittivity and decrease the effective thickness of pristine friction PDMS which further resulted in enhancement of output performance. In precursor emulsion, high stirring speed endowed liquid with high shear force, which would induce small size of droplets as both dispersed and continuous phase were

deformable.[31, 33, 36] Correspondingly, the interfacial area could be enlarged by such method, which was much more convenient than the preparation of solid doping materials with different sizes. Besides, according to our previous work, the liquid micro-droplets could be applied as functional molecules micro-carrier to tailor its interfacial properties, which avoided chemical reaction by simply dissolution of functional molecules.[29] Typically, surfactants with distinct polarity groups in their tails and head were the powerful functional molecules to adjust liquid-liquid interfacial compatibility in emulsion, which was introduced by simply dissolution. The concepts have been widely applied in emulsion polymerization and have been proved with its success.[31-34, 37-39] Herein, we introduced the concepts of emulsion dispersed system to the PDMS encapsulated high permittivity liquid composite with the aim for studying the relationship between the interface and triboelectric performance and exploiting it to maximize the output performance of liquid filling composite.

2.2 Interfacial modification to enhance triboelectric performance of liquid doping materials.

2.2.1 Enlarge interfacial area via high preparation stirring speed.

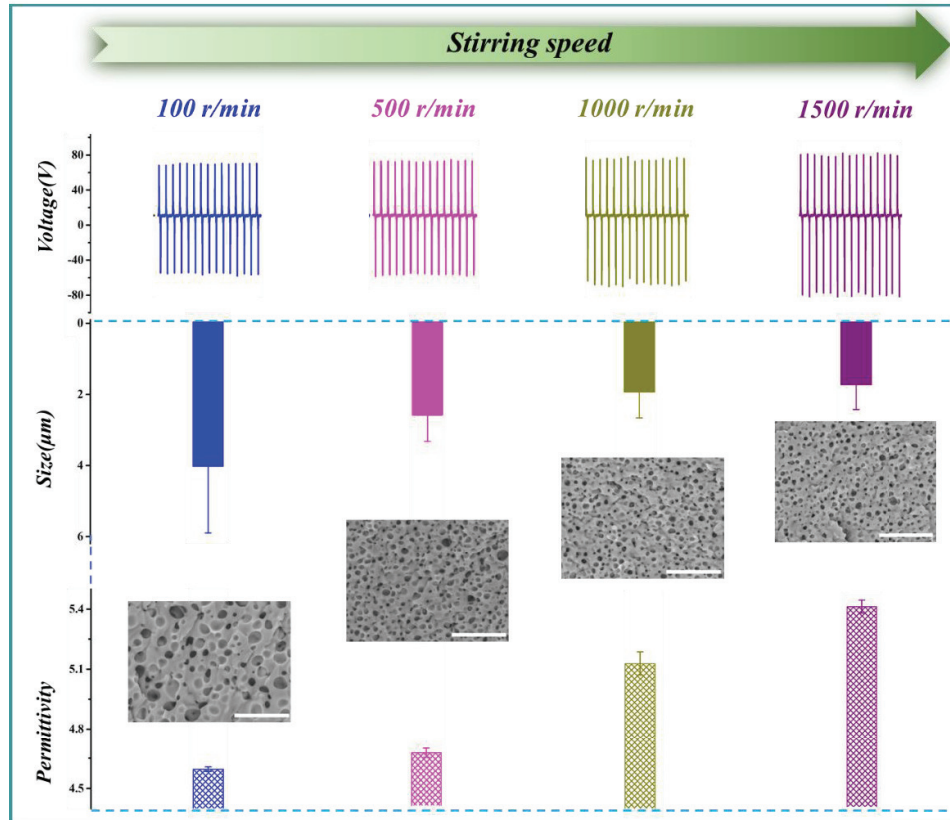


Figure 2. The influence of preparation stirring speed on the PDMS-HD30 films' properties, such as output voltage, PDMS-HD30 composite pores' size and their inner region SEM images, corresponding permittivity. The scale bars of SEM images were 30 μm .

The interfacial area's influence was firstly investigated as it could be conveniently tailored by preparation stirring speed in our liquid doping PDMS and could exclude other external factors on composites, which thereby endowed us with clear understating about the correlation between droplets interfacial area and composites' properties.[33, 34] Fig 2 presented the relationship between preparation stirring speed and properties of PDMS composites with 30% mass filling ratio of high permittivity liquid (PDMS-HD30). The triboelectric performances were measured by a self-made vertical contact-separation mode TENG of 15.2 cm^2 contact area to uniformly compare all PDMS composites, which was applied with a periodical force of 100 N at a frequency of 3 Hz. The details of TENG test were presented in the experiment section. As expected, the

output performance of PDMS-HD30 exhibited a proportional correlation to stirring speed. At 100 r/min, the output voltage of PDMS-HD30 was 68 V. As the applied stirring in fabrication became vigorous, the output voltage increased with the stirring speed from 71 V at 500 r/min, 82 V at 1,000 r/min, to 94 V at 1,500 r/min. The corresponding current and transfer charge also exhibited similar relationship with stirring speed, 2.01 μ A, 2.71 nC/cm² at 100 r/min, 2.19 μ A, 3.06 nC/cm² at 500 r/min, 2.35 μ A, 3.42 nC/cm² at 1,000 r/min, to 3.03 μ A, 4.19 nC/cm² at 1,500 r/min, which was shown in Tab S1 and Fig S2. However, higher stirring speed (>1,500 r/min) would bring frictional heat generation in emulsion precursor and even induced curing of PDMS pre-cured solution which could not be stirred. The maximum preparation stirring speed was thus limited to 1,500 r/min in this work and the prepared composite showed enhancement of 38% in output voltage, 51% in output current and 54% in transfer charge as compared to that of 100 r/min prepared PDMS-HD30 composites. Meanwhile, it was observed that PDMS-HD30 composites' permittivity was gradually enhanced with the preparation stirring speed, which were 4.58 \pm 0.01 at 100 r/min, 4.64 \pm 0.02 at 500 r/min, 5.06 \pm 0.05 at 1,000 r/min and 5.31 \pm 0.03 at 1,500 r/min respectively, as shown in Fig 2. As no other changes were employed on composites, the triboelectric performance enhancement was consequently attributed to the permittivity enhancement because the enhanced permittivity boosted the capability of charge store in friction materials and further improved its triboelectric performance as stated in aforementioned paragraph. Furthermore, considering that the filling ratios of all composites were same

and fixed at 30%, the enhanced composites' permittivity was originated from inner structures change of composites which resulted from preparation stirring speed.

To further figure out the essence of the stepwise enhanced composites' permittivity as well as triboelectric performance, SEM was conducted on these film to observe their structures. As shown in Fig 2 and S3 to S6, large amount of pores was observed in cross-section images of composites which were originated from the occupied space of droplets. The high permittivity liquid droplets replaced the inner friction PDMS, resulting permittivity increase of PDMS composite and effective thickness decrease of pristine PDMS. The capacitance of friction composites was enhanced, which further induced improvement of triboelectric performance. Besides, droplets in all PDMS-HD30 composites showed similar inhomogeneous distribution, which was found that there were limited pores in upper region as closed to the friction surface. The effective contact area of friction PDMS was not reduced because no PDMS in the surface was replaced by the doping material, which benefits to tribo-electrification. Notably, the sizes of pores showed an inverse correlation to the preparation stirring speed. As higher stirring speed was employed to the fabrication of PDMS-HD30 composites, the size of pores gradually decreased from $4.09 \pm 1.86 \mu\text{m}$ at 100 r/min, $2.64 \pm 0.72 \mu\text{m}$ at 500 r/min, $1.99 \pm 0.71 \mu\text{m}$ at 1,000 r/min, to $1.79 \pm 0.69 \mu\text{m}$ at 1,500 r/min. The corresponding interfacial area was thus enhanced. Meanwhile, the permittivity of PDMS-HD30 exhibited gradual increase as the stirring became vigorous. As no additional factors were introduced in such dispersed system, the permittivity increase was believed to be decided by the enlarged interfacial area with higher polarization levels, dielectric

response and breakdown strength, which was agreed well with other reported works.[23, 40-42] However, the permittivity increase was not linearly correlated to droplets' size decrease. The permittivity increases slightly from 4.58 ± 0.01 to 4.64 ± 0.02 when the droplets' size was reduced from $4.09 \pm 1.86 \mu\text{m}$ at 100 r/min to $2.64 \pm 0.72 \mu\text{m}$ at 500 r/min and it became obvious as the droplets' size was further reduced from $1.99 \pm 0.71 \mu\text{m}$ at 1,000 r/min. The transparency of PDMS-HD30 also increased with the stirring speed, as shown in Fig S2. With the high stirring speed, the size distribution of dispersed droplets became homogeneous and further alleviated the optical scattering in emulsion. The transparency of PDM-HD was enhanced in consequence, which was 63% at 100 r/min, 70% at 500 r/min, 71% at 1,000 r/min and to 77% at 1,500 r/min. These results illustrated that small size of droplets with large interfacial area would be beneficial to the permittivity as well as output performance of liquid doping PDMS composite and the effect was more obviously when the size of droplets were in a small region.

2.2.2 Improve interfacial compatibility via surfactant introduction.

The increase of interfacial area had proved its value in composites' permittivity and triboelectric performance. Moreover, the interface compatibility was subsequently investigated by Span 20 surfactant additive which improved the interfacial compatibility as we stated in aforementioned paragraph. For a comparable study with interfacial area influence, the preparation stirring speed in compatibility study of composites were fixed to 100 r/min.

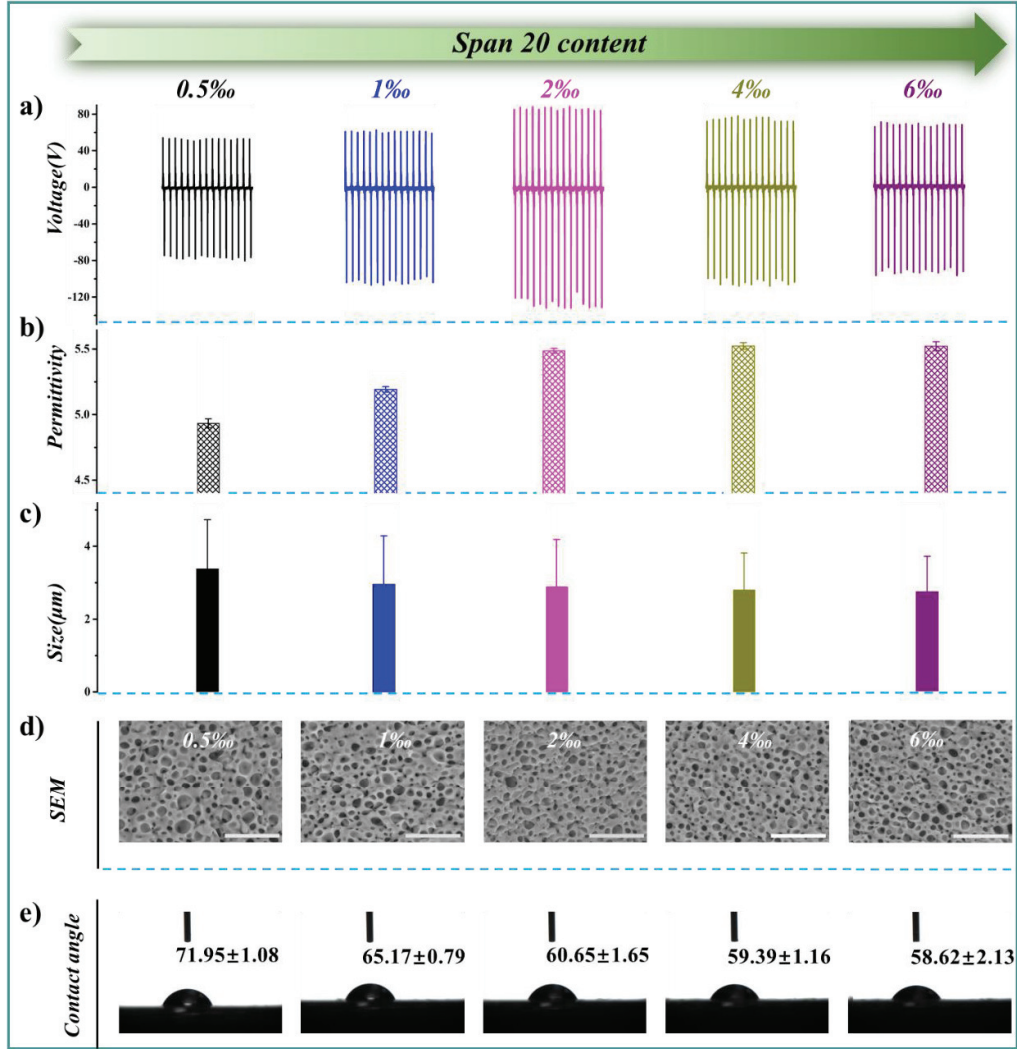


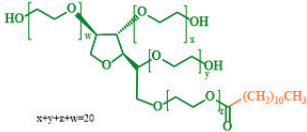
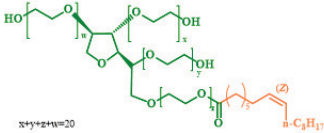

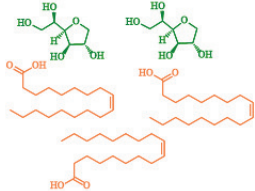
Figure 3. The influence of Span 20 additive's contents on PDMS-HD30 films' properties. a) output voltage, b) permittivity, c) PDMS-HD composite pores' size, d) inner region SEM images of corresponding PDMS-HD composite films. The scale bars were 30 μm . e) **Contact angle between PDMS film and high permittivity liquid with different contents of Span 20 additive.**

The influence of different Span 20 additive's contents on PDMS-HD films' properties was presented in Fig 3. As the Span 20 content was increased to 2‰, the output voltage was gradually enhanced from 68 V at non additive to 132 V. The transfer charge and output current also exhibited similar tendency, as shown in Fig S7 and Tab S2. Meanwhile, the permittivity was stepwise improved from 4.58 ± 0.01 at non additive,

4.93±0.03 at 0.5‰, 5.19±0.02 at 1‰, to 5.49±0.02 at 2‰. The corresponding droplets' size also changed with the Span 20 additive content, which was decreased from 4.09±1.86 μm at non additive, 3.38±1.34 μm at 0.5‰, 2.96±1.32 μm at 1‰, to 2.89±1.30 μm at 2‰, as shown in Fig 3, S8, S9 and S10. According to the results of interfacial area's influence on permittivity in aforementioned paragraph, the contribution to permittivity enhancement from corresponding enlarged interfacial area was slight as all samples' droplets size were larger than 2.64±0.72 μm. The permittivity enhancement thus was attributed to the improvement of interfacial compatibility, which improve the interfacial polarization with decreasing negative effects and consequently affording high permittivity.[22, 23] With more Span 20 was added to the system, the composites' permittivity became steady. The reason was that the interface was saturated by Span 20 when the content was above 2‰ and the additional Span 20 was existed in inner region which no longer promoted the interface compatibility. The contact angle between PDMS film and high permittivity liquid with different Span 20 additive's contents confirmed the speculate, as shown in Fig 3e and S13. The contact angle decreased from 74.97±1.23° at non additive to 60.65±1.65° at 2‰ Span 20 additive, indicating that the liquid-PDMS interface compatibility was significantly improved. However, the contact angle did not show obvious declining when more Span 20 was added, 59.39±1.16° at 4‰ and 58.62±2.13° at 6‰ and the interface compatibility thus was not improved significantly. Unfortunately, the output voltage was not steady and gradually decreased to 99 V at 6‰. It should be pointed that surfactant could be applied as antistatic agent, which undermined the tribo-electrification charge. When high

content of Span 20 was introduced in the composites, the redundant surfactant thus deteriorated the output performance. In order to further present the effect of surfactant on triboelectric performance, Span 20 was directly added to PDMS without high permittivity liquid doping. As shown in Fig S14, the PDMS's output performance was stepwise decrease as the Span 20 content was increased to 6‰ and the permittivity of PDMS was maintained, which manifested the antistatic effect of Span 20. The antistatic agent role of surfactant limited the enhancement of triboelectric performance of liquid doping materials and the optimal content of Span 20 was determined to 2‰ in this work. The surfactant additive proved that the improvement of interfacial compatibility would promote PDMS-HD30's permittivity as well as triboelectric performance. Besides, the transparency of PDMS-HD30 was increased with Span 20 additive content owing to the homogeneous distribution of droplets' size, as shown in Fig S7.

Table 1. The chemical structure and HLB of surfactants and corresponding PDMS-HD30 composites' output voltage.

Surfactant	Chemical structure	HLB	Output voltage
Tween 20	 $x+y+z+w=20$	16.7	87 V
Tween 80	 $x+y+z+w=20$	15	76 V
Span 20		8.6	105 V
Span 83		3.7	91 V

The Span 20 additive had demonstrated the importance of interfacial compatibility in composites' triboelectric performance. However, the types of surfactants are numerous, which are of different abilities in improving interfacial compatibility. Other surfactants, Span 83, Tween 20 and Tween 80, which have similar chemical group but of different Hydrophile Lipophilic Balance (HLB) values, were employed as additive to improve the interfacial compatibility and further investigate the inner relationship with triboelectric performance. The content of such surfactants were determined to 1% in high permittivity liquid as Tween was found to inhibit the cured process of PDMS at high content in this work. As expected, all these surfactants additive in liquid boosted the output performance of composites. The output voltages and transfer charges of composites were displayed in Fig 3, Fig S15 and Tab 1. The output voltage of

composites with Tween 80, Tween 20 and Span 83 additive were 87 V, 76 V and 91 V, which were all higher than it of PDMS-HD30 without surfactant additive. The transfer charge and output current exhibited similar enhancement tendency. On the basis of the results we discussed in above paragraph, the enhancement could be explained from the increase of interfacial compatibility. Nonetheless, the ability of surfactants in improvement of the interfacial compatibility as well as triboelectric performance was varied as HLB of surfactants changed. In precursor emulsion, the high permittivity liquid was a high polarity liquid which was encapsulated by low polarity PDMS pre-cured liquid. The precursor emulsion was similar with typical W/O emulsion, in which high permittivity liquid with high polarity replaced the role of water. The lipid-soluble surfactants with $HLB \leq 10$ thereby would be more suitable to stabilize such emulsion system with compatible interface and the output voltage results manifested that the performance of water-soluble Tween additive was inferior to that of lipid-soluble Span additive. In addition, it was notable that Span 20 render a better performance than Span 83 in the improvement of output performance, even Span 20 with 8.6 HLB value is less lipid-soluble than Span 83 with 3.7 HLB value. For Span 83, extremely low HLB usually meant that surfactant possessed large lipid-solubility group and small water-solubility group in each end of chemical structure. The encapsulated high polarity liquid of droplets was not with enough ability to drag all surfactant of extremely low HLB into the interface as the small water-solubility group. The improvement of interface compatibility by extremely lipid-soluble surfactant was consequently lower than that of surfactant with appropriate HLB value. The results implied that HLB of surfactant

should be harmonious with the two phase polarity difference. Generally, all these surfactants were inferior to Span 20 in this work which was the best in the improvement of output performance at same concentration. Nonetheless, it should be pointed that other surfactants also possess the ability to enhance the compatibility of interface. The numerous kinds of surfactants will bring in numerous interesting phenomena in interface modified doping composites which are valuable to explore. However, only two typical surfactants were studied in this work and the other surfactants were not presented due to the limited length of this work.

2.3 Comprehensive interfacial modification in PDMS-HD with optimal properties

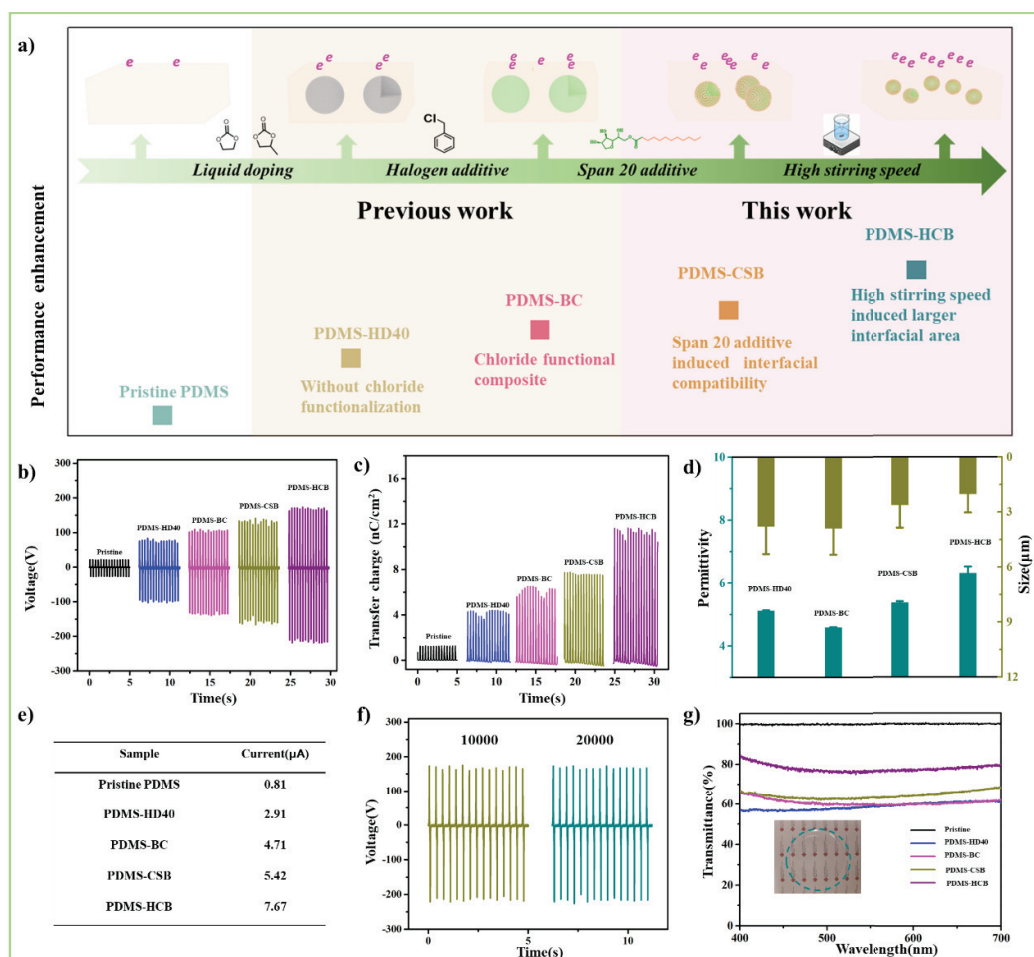


Figure 4. Stepwise prepared high performance liquid doping PDMS composites PDMS-HD40, PDMS-BC, PDMS-CSB and PDMS-HCB as well as their properties. a) Scheme of prepared protocol. b) Output voltage. c) Transfer charge. d) Permittivity and dispersed liquid droplets' size. e) Output current. f) Durability test of PDMS-HCB after 15,000, 20,000 cycles. g) Transmittance of PDMS composites.

Based on the aforementioned results, we employed the interfacial modification by comprehensive methods to maximize the output performance of the liquid doping composites. The scheme and results were depicted in Fig 4. In principle, the permittivity of composites had a strong correlation with the filling ratio of high permittivity materials.[17] The mass ratio of high permittivity liquid was increased to 40% for enhancement of composites permittivity and the output performance, which was termed as PDMS-HD40. The PDMS-HD40 had higher droplets density in composites than it of PDMS-HD30 as higher ratio liquid was introduced, as shown in Fig S16. When PDMS-HD40 was fabricated at the stirring speed of 100 r/min, the droplet's size and distribution was similar with that of PDMS-HD30, indicating the droplet's size and distribution were steady with the same preparation stirring speed. The PDMS-HD40 composite's permittivity reached 5.12 ± 0.01 and corresponding output voltage was improved to 103 V, which was 50% enhancement as compared to PDMS-HD30's output voltage. To further improve the output performance of composites, 6% benzyl chloride additive was subsequently introduced to the high permittivity liquid since halogens were reported as good electron affinity and the prepared composite was called as PDMS-BC.[43, 44] The chloride functional composite featured higher electron affinity and resulted in higher output performance, which had been presented in our previous work.[29] As shown in Fig 4d, S16 and S17, the size of droplets' was steady at same preparation stirring speed when benzyl chloride was introduced. The PDMS-BC

composite's permittivity decrease resulted from the introduction of low permittivity of benzyl chloride in doping liquid. However, the higher electron affinity improved the composite's output voltage to 140 V, which was 36% improvement as compared to PDMS-HD40 composite without benzyl chloride additive. Furthermore, 2‰ Span 20 was added to the benzyl chloride high permittivity solution for the purpose of improvement of interfacial compatibility and the prepared composite was termed as PDMS-CSB. The permittivity of such PDMS-CSB composite was enhanced to 5.37 ± 0.04 and the output voltage was further enhanced to 166 V. Finally, the stirring speed in fabrication increased to 1,500 r/min and the prepared composite was called as PDMS-HCB. The PDMS-HCB composite permittivity achieved a higher value of 6.30 ± 0.21 on the basis of PDMS-CSB, demonstrating synergistic interfacial effect by stirring speed and Span 20 additive in composite permittivity enhancement. The output voltage of PDMS-HCB was 219 V, which also showed an enhancement as compared to PDMS-CSB. The corresponding transfer charge and output current were observed with similar tendency with output voltage in all composites. In general, the total enhancement of such PDMS-HCB composites was 8.1 folds in output voltage, 9.5 folds in output current, 9.1 folds in transfer charge as compared to pristine PDMS. The significantly enhancement in output performance demonstrated the interfacial modification's promising potentials in doping composites of triboelectric materials for energy harvesting and it should be taken into comprehensive consideration in doping triboelectric composites as the different effects which brought from interfacial modification.

The other properties of composites were also presented in Fig 4. The composites durability test was performed on representative PDMS-HCB composite, which was displayed in Fig 4f. After 10,000 and 20,000 cycles, the output voltage of PDMS-HCB presented a steady performance, illustrating that PDMS-HCB was durable composites in friction materials. The transparence of these films in visible region (400~700 nm) were exhibited in Fig 4g. PDMS-HD40 appeared inferior transparence as compared to PDMS-HD30, due to the high filling ratio of liquid in composites along with high visible optical scattering. It was notable that the transparence increased via aforementioned treatment in PDMS-HD40 of surfactant additive and vigorous stirring. The transmittances of composites films were measured as 59% of PDMS-HD40, 60% of PDMS-CB, 63% at PDMS-CSB and 76% of PDMS-HCB. Owing to the high output performance as well as transparency of PDMS-HCB, the following tests were performed on such composites. The stretchability of PDMS-HCB film was evaluated by a $3 \times 0.5 \text{ cm}^2$ sample. As shown in Fig S20, under applied tensile force, the sample could be stretched over 6 cm which was calculated with over 100% of stretchability. These results manifested that the composite was a transparent and stretchable material.

Other test conditions of different applied force and frequency were also employed to assess the output performance of PDMS-HCB composite. The applied force of 100 N was fixed to study the impact of frequency on output voltage at first. As depicted in Fig S21, the output voltage increased with the increasing frequency, 155 V at 1 Hz, 190 V at 2 Hz and 300 V at 3.4 Hz. The results illustrated that the composites featured excellent output voltage at low-frequency which was suitable in wearable power source.

Subsequently, the applied frequency was fixed at 3 Hz but with different applied forces. The output voltages were shown in Fig S22 and exhibited a proportional relation with applied force, 159 V at 50 N, 280 V at 150 N and 317 V at 200 N respectively. The proportional tendency indicated that the composites could be adapt to wide range of force and made it promising in the environment with complex external force.

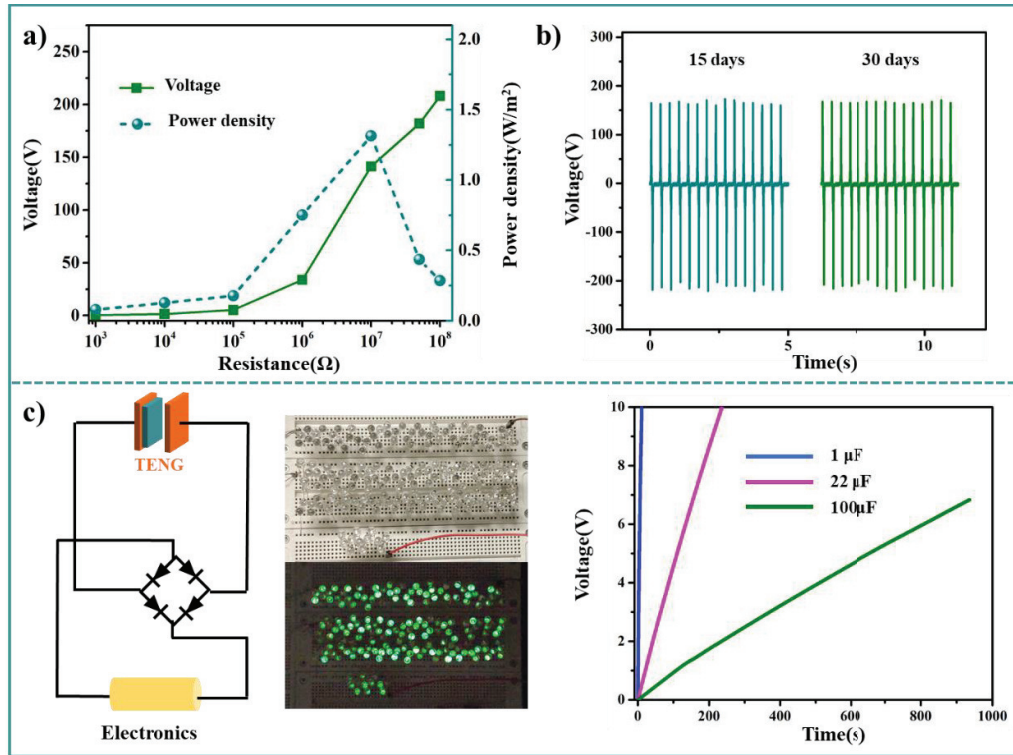


Figure 5. a) The output voltage and instantaneous power density of PDMS-HCB assembled TENG at different external load resistance. b) Stability test of PDMS-HCB after 15 days and 30 days. c) The circuit of driving electronics, in which PDMS-HCB assembled TENG was the power source. The demonstration included the lighting of 176 green LEDs and capacitor charging curve (voltage *versus* time).

To further investigate the PDMS-HCB capability as a power source, different external loads were connected to the assembled TENG in series circuit, as shown in Fig 5. Resistors of different resistance values (10^3 – 10^8 Ω) were firstly applied to evaluate the output voltage and instantaneous power density, as shown in Fig 5a. The curve of

resistors *versus* output voltage demonstrated that the output voltage increased with the increasing resistance and 210 V of output voltage was measured as the external resistance reached to $10^8 \Omega$. The instantaneous power density was calculated from $W=V^2/R$ and the peak value was reached when the external $10^7 \Omega$ resistor was connected to the series. Furthermore, the output stability of such composites was also demonstrated by recording of the output voltage at different days. As shown in Fig 5b, the output voltage was measured as a stable number of around 210 V and showed negligible fluctuation at tested time of 15 days and 30 days. 176 green LEDs were further directly connected to the TENG to exhibit its ability of powering electronics. As shown in Fig 5c, the LEDs were lightened by the TENG in good brightness. Finally, capacitors of 1 μF , 22 μF and 100 μF were utilized to store electricity which was generated from the TENG for demonstrating the TENG's ability of power source. The output signal generated from TENG was adjusted by a bridge rectifier to charge the capacitors. The capacitors charging curve was shown in Fig 5c and the gradually increasing voltage of capacitors indicated that the capacitors could be charged by the TENG successfully. The capacitor of 1 μF could be charged to 10 V within 11 s at the rate of around 906 mV/s. As for 22 μF and 100 μF capacitor, the charging rates were 42 mV/s and 7 mV/s respectively. The increase of capacitors voltage proved the promising potential of PDMS-HCB in friction materials.

2.4 Flexible TENG for gesture detection and energy harvesting

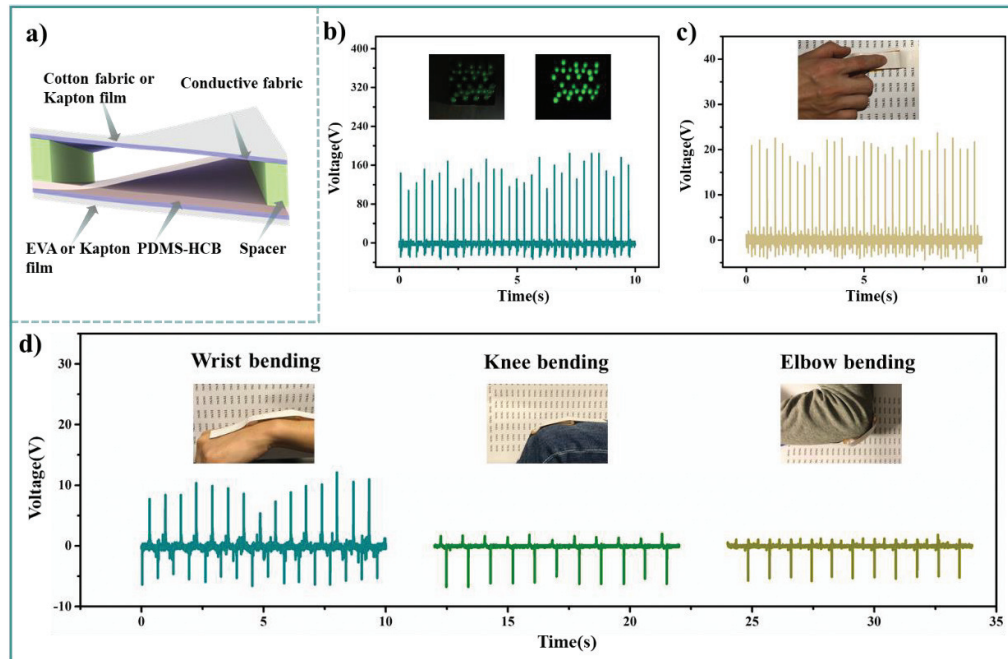


Figure 6. a) The structure of flexible TENG prepared from PDMS-HCB. b) Output voltage of flexible TENG when it was flapped by hand and 30 green LEDs were powered up. Electric signals generated from flexible TENG by c) finger tapping, d) bending of wrist, knee and elbow.

The PDMS-HCB composite with high triboelectric performance and flexibility was further applied to fabricate flexible TENG with the purpose of biomechanical energy harvesting. Cotton fabric and black EVA film (ethylene vinyl acetate copolymer) were used as frame of the flexible TENG device because the flexibilities of cotton fabric and EVA make them comfortable when they were touched by human skin. The devices of flexible TENG are also similar with our previous work except the applied friction materials in TENG.[29] As the new composites was applied, the corresponding TENG exhibited a better performance. As shown in Fig 6a, the PDMS-HCB film was adhered to back electrode of conductive fabric and then fixed on the EVA film with the assistance of double sided adhesive tape. The cotton fabric which was coupled with another piece of conductive fabric was then employed as top support substrate for the

flexible TENG and elastic sponges supplied the TENG with around 4 mm space between the cotton/conductive fabric and EVA film, as shown in Fig 6a. By tapping the flexible TENG, the composite film and conductive fabric was brought to contact and separation and the output voltage signal was thus observed, which was generated from the TENG and could reach as high as 180 V. 30 green LEDs were connected to the flexible TENG in circuit, for the demonstration of the flexible TENG's potential in powering electronic device. As exhibited in Fig 6b, 30 green LEDs were lightened up by the electricity generated from the flexible TENG when it was tapped. These results rendered that the flexible TENG was efficient in biomechanical energy harvesting.

The PDMS-HCB composite also possessed potentials in e-skin applications owing to its flexibility and high output performance. For instance, the film of such composite was employed for fabrication of self-power human moving gesture detective TENG device (Ges-TENG) in this work which had similar structure with the aforementioned flexible TENG. However, two $1.5 \times 7 \text{ cm}^2$ thin Kapton films were applied as top and bottom support substrates of Ges-TENG instead of EVA because Kapton films are more flexible. A piece of $1.2 \times 6 \text{ cm}^2$ conductive fabric was adhered to the film of composite, which was the electronegative material and corresponding back electrode, respectively. The two Kapton substrates were connected by two spaces of 1 mm thickness. As the high flexibility of used materials, Ges-TENG featured excellent flexibility. Moreover, the high output performance of composites endowed Ges-TENG with high sensitivity in human gesture detection. As illustrated in Fig 6c and 6d, Ges-TENG was applied in different moving parts of body such as finger, wrist, elbow and knee to detect human

moving gesture. Under iterative bending-stretching cycles of human gesture, the top and bottom substrates were brought into contact and separation which induced output signal from Ges-TENG. The gesture was thereby detected by oscilloscope without additional energy supplement. In the detail of finger tapping, Ges-TENG produced an output voltage signal of as high as 20 V when it was tapped. The other moving parts of body could be also detected by Ges-TENG, exhibiting Ges-TENG's ability of recognition of human body part movements.

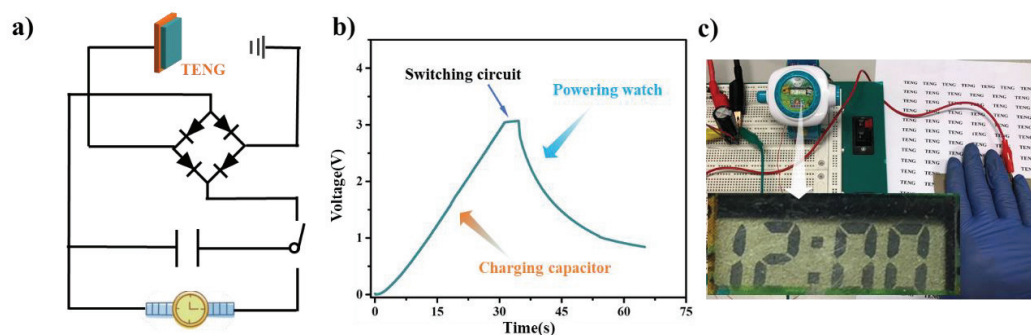


Figure 7. a) The structure of flexible single electrode TENG and circuit of powering watch. b) The voltage of capacitor in charging process and powering process. c) Image of circuit and working watch.

The PDMS-HCB composites could be applied to fabricate flexible TENG of single electrode power source, which was further used to power an electric watch. As shown in Fig 7, PDMS-HCB composites film was adhered to conductive fabric to assemble single electrode TENG and then connected to the designed circuit. Via continuous tapping on the PDMS-HCB, the electricity was generated and used to charging 22 μ F capacitor. The charging process lasted for around 30 s and after that the circuit was adjusted by hand switching to power the electric watch. The electric watch was thereby powered by the electricity in the capacitor which was harvest from hand tapping. The

working time of watch was around 20 s and the screen of time could be clearly seen in Fig 7c.

3. Conclusion

In conclusion, the concept of interfacial modification, including enlarged interfacial area and compatible interface between doping materials and friction matrix, was introduced into doping friction composites of TENG. The enlarged interfacial area was achieved by simply high preparation stirring speed and interface compatibility could be improved by appropriate surfactant additive in the liquid doping friction PDMS composites, which avoided complex preparation of different size filler and chemical surface modification in solid doping materials. The interfacial modification could afford higher composites permittivity and further enhance friction composites' triboelectric performance. The prepared PDMS-HCB composites' output performance was improved obviously on the basis of non-modified PDMS-HD40 and the total enhancement was achieved as 8.1-fold in output voltage and 9.5-fold in output current of pristine PDMS. The corresponding TENG could light 176 green LEDs as well as charge capacitors. Moreover, PDMS-HCB was also employed in flexible TENG which was used to detect movement of human body's moving parts. This work revealed the great value of interfacial modification in the doping friction composites for improvement of triboelectric performance and much effort should be committed to the interface issue when new doping materials was introduced in friction materials.

4. Experiment section

Materials and Characterization

Propylene carbonate (PC) and ethylene carbonate (EC) were purchased from Alfa Aesar. PDMS (Sylgard 184) was obtained from Dow Corning. Span 20, Span 83, Tween 20, Tween 80 and benzyl chloride were the products of Dieckmann company. Conductive fabric was Cu/Ni coated fabric which was bought from 3 M Corp. All reagents were used as received without further purification.

Triboelectric performance test was conducted on button/key durability life test machine, ZX-A03, zhongxingda Shenzhen. Oscilloscope of keysight infiniivision DSOX3024T was used to record the output voltage. Electrometer of Keithley 6514 system of Tektronix, Inc was applied to measure the output current and transfer charge. The transmittance of film was measured by Hitachi UH5300. Hitachi TM-3000 was applied to observe the structure of films. The films' permittivity were calculated from their capacitance, $C = \varepsilon_0 * S \frac{\varepsilon_r}{d}$. LCR-6300, 300kHz, GW Instek was employed to the capacitance measurement. The contact angle was measured from SDC-350 of dynetech, Guangdong.

High permittivity liquid and PDMS solution

High permittivity liquid was the mixed liquid of EC and PC at 4:1 volumetric ratio.[45] PDMS solution was the mixture of elastomer and curing agent at recommended mass ratio of 10:1 from the company.

Fabrication of PDMS-HD composites film at different stirring speed

The PDMS solution was weighted at first. High permittivity liquid was then added to PDMS solution at mass ratio of 30 % (PDMS-HD30) or 40%(PDMS-HD40). The mixture was stirred by mechanical stirring for 15 mins at designed stirring speeds of 100 r/min, 500 r/min, 1000 r/min or 1500 r/min, respectively. The mixture became sticky and the emulsion was thus formed. The emulsion was poured in petri dish mold in designed thickness of around 540 μm . After that, the mold was heated at 70°C for 3 h in oven to cure the emulsion. The film was obtained by peeling off when it was cold in air.

Fabrication of PDMS-HD composites film with surfactant additive

The surfactant was dissolved in high permittivity liquid at designed concentration. The Span 20's concentrations were 0.5‰, 1‰, 2‰, 4‰ and 6‰. The concentrations of other surfactants Span 83, Tween 20 and Tween 80 were determined to 1‰. The high permittivity liquid with surfactant additive was then stirred with PDMS solution of 30% mass ratio at speed of 100 r/min. The cured process was same with PDMS-HD composites film.

Chloride functional PDMS-BC composites film

Benzyl chloride was dissolved in high permittivity liquid at 6% concentration for use. The liquid with benzyl chloride additive was mixed with PDMS solution of 40% mass ratio at the speed of 100 r/min for 15 min. The cured process was same with PDMS-HD composites film.

PDMS-CSB and PDMS-HCB composites film

Span 20 was added to the benzyl chloride solution at 2‰ concentration. The prepared liquid was mixed with PDMS solution of 40% mass ratio at the speed of 100 r/min (PDMS-CSB) or 1,500 r/min (PDMS-HCB) for 15 mins. The cured process was same with PDMS-HD composites film.

Assemble vertical contact-separation mode TENG for test.

The TENG was assembled as our previous work.[29] In detail, two $9\times 8\times 0.5\text{ cm}^3$ separated polymethyl methacrylate (PMMA) substrates were applied as frame of TENG, with sponges on the four corners as spacer. Another circular PMMA substrate of 4.4 cm diameter was covered by conductive fabric and adhered to the top PMMA substrate subsequently. The space between conductive fabric and bottom PMMA substrate was 5 mm. The conductive fabric on circular PMMA substrate was used as electropositive friction materials. The PDMS or PDMS composites films were electropositive friction materials and another piece of conductive fabric was combined as back electrode. The PDMS or PDMS composites films with back electrode was then adhere to the bottom PMMA substrate for test. All test conditions were fixed at 100 N with frequency of 3 Hz unless specified.

Acknowledgements

The authors acknowledge The Hong Kong Polytechnic University (G-YBV2) for funding supports of this work.

References:

- [1] F.R. Fan, W. Tang, Z.L. Wang, *Advanced Materials*, 28 (2016) 4283-4305.
- [2] X. Cao, Y. Jie, N. Wang, Z.L. Wang, *Advanced Energy Materials*, 6 (2016).
- [3] J. Zou, M. Zhang, J. Huang, J. Bian, Y. Jie, M. Willander, X. Cao, N. Wang, Z.L. Wang, *Advanced Energy Materials*, 8 (2018).
- [4] W. Tang, T. Jiang, F.R. Fan, A.F. Yu, C. Zhang, X. Cao, Z.L. Wang, *Advanced Functional Materials*, 25 (2015) 3718-3725.
- [5] X. Guan, B. Xu, J. Gong, *Nano Energy*, 70 (2020).
- [6] F.-R. Fan, Z.-Q. Tian, Z. Lin Wang, *Nano Energy*, 1 (2012) 328-334.
- [7] C. Wu, A.C. Wang, W. Ding, H. Guo, Z.L. Wang, *Advanced Energy Materials*, 9 (2019).
- [8] B. Yang, W. Zeng, Z.-H. Peng, S.-R. Liu, K. Chen, X.-M. Tao, *Advanced Energy Materials*, 6 (2016).
- [9] Q. Zheng, L. Fang, H. Guo, K. Yang, Z. Cai, M.A.B. Meador, S. Gong, *Advanced Functional Materials*, 28 (2018).
- [10] C. Yao, A. Hernandez, Y. Yu, Z. Cai, X. Wang, *Nano Energy*, 30 (2016) 103-108.
- [11] K. Parida, V. Kumar, W. Jiangxin, V. Bhavanasi, R. Bendi, P.S. Lee, *Adv Mater*, 29 (2017).
- [12] J. Gong, B. Xu, X. Tao, *ACS Appl Mater Interfaces*, 9 (2017) 4988-4997.
- [13] J. Gong, B. Xu, X. Guan, Y. Chen, S. Li, J. Feng, *Nano Energy*, 58 (2019) 365-374.
- [14] R. Wen, J. Guo, A. Yu, J. Zhai, Z.L. Wang, *Advanced Functional Materials*, 29 (2019).
- [15] A. Yu, Y. Zhu, W. Wang, J. Zhai, *Advanced Functional Materials*, (2019).
- [16] S. Niu, S. Wang, L. Lin, Y. Liu, Y.S. Zhou, Y. Hu, Z.L. Wang, *Energy & Environmental Science*, 6 (2013).
- [17] J. Chen, H. Guo, X. He, G. Liu, Y. Xi, H. Shi, C. Hu, *ACS Appl Mater Interfaces*, 8 (2016) 736-744.
- [18] J. Kim, H. Ryu, J.H. Lee, U. Khan, S.S. Kwak, H.J. Yoon, S.W. Kim, *Advanced Energy Materials*, 10 (2020).
- [19] R. Wen, J. Guo, A. Yu, K. Zhang, J. Kou, Y. Zhu, Y. Zhang, B.-W. Li, J. Zhai, *Nano Energy*, 50 (2018) 140-147.
- [20] X. Xia, J. Chen, H. Guo, G. Liu, D. Wei, Y. Xi, X. Wang, C. Hu, *Nano Research*, 10 (2016) 320-330.
- [21] B. Fan, M. Zhou, C. Zhang, D. He, J. Bai, *Progress in Polymer Science*, 97 (2019).
- [22] H. Luo, X. Zhou, C. Ellingford, Y. Zhang, S. Chen, K. Zhou, D. Zhang, C.R. Bowen, C. Wan, *Chem Soc Rev*, 48 (2019) 4424-4465.
- [23] Z.M. Dang, J.K. Yuan, S.H. Yao, R.J. Liao, *Adv Mater*, 25 (2013) 6334-6365.
- [24] S.A. Paniagua, Y. Kim, K. Henry, R. Kumar, J.W. Perry, S.R. Marder, *ACS Appl Mater Interfaces*, 6 (2014) 3477-3482.
- [25] X. Du, Y. Liu, J. Wang, H. Niu, Z. Yuan, S. Zhao, X. Zhang, R. Cao, Y. Yin, N. Li, C. Zhang, Y. Xing, W. Xu, C. Li, *ACS Appl Mater Interfaces*, 10 (2018) 25683-25688.
- [26] G.Z. Li, G.G. Wang, D.M. Ye, X.W. Zhang, Z.Q. Lin, H.L. Zhou, F. Li, B.L. Wang, J.C. Han, *Advanced Electronic Materials*, 5 (2019).

- [27] J.-G. Sun, T.N. Yang, I.S. Kuo, J.-M. Wu, C.-Y. Wang, L.-J. Chen, *Nano Energy*, 32 (2017) 180-186.
- [28] V. Harnchana, H.V. Ngoc, W. He, A. Rasheed, H. Park, V. Amornkitbamrung, D.J. Kang, *ACS Appl Mater Interfaces*, 10 (2018) 25263-25272.
- [29] T. Jing, B. Xu, Y. Yang, *Nano Energy*, 74 (2020).
- [30] P. Mazurek, L. Yu, R. Gerhard, W. Wirges, A.L. Skov, *Journal of Applied Polymer Science*, 133 (2016).
- [31] C. Chern, *Progress in polymer science*, 31 (2006) 443-486.
- [32] Y. Morishita, H. Morita, D. Kaneko, M. Doi, *Langmuir*, 24 (2008) 14059-14065.
- [33] R. Pal, *AIChE Journal*, 42 (1996) 3181-3190.
- [34] A. Soottitantawat, H. Yoshii, T. Furuta, M. Ohkawara, P. Linko, *Journal of Food Science*, 68 (2003) 2256-2262.
- [35] R. Simpkin, *IEEE Transactions on Microwave Theory and Techniques*, 58 (2010) 545-550.
- [36] W.V. Smith, R.H. Ewart, *The journal of chemical physics*, 16 (1948) 592-599.
- [37] T. Jing, T. Li, Z. Ruan, L. Yan, *Journal of Materials Science*, 53 (2018) 14933-14943.
- [38] T. Jing, T. Li, Z. Ruan, Q. Cheng, L. Yan, *Macromolecular Materials and Engineering*, 303 (2018).
- [39] T. Zhang, R.A. Sanguramath, S. Israel, M.S. Silverstein, *Macromolecules*, 52 (2019) 5445-5479.
- [40] Q. Wang, L. Zhu, *Journal of Polymer Science Part B: Polymer Physics*, 49 (2011) 1421-1429.
- [41] P. Murugaraj, D. Mainwaring, N. Mora-Huertas, *Journal of Applied Physics*, 98 (2005).
- [42] J. Li, *Phys Rev Lett*, 90 (2003) 217601.
- [43] L. Chen, Q. Shi, Y. Sun, T. Nguyen, C. Lee, S. Soh, *Adv Mater*, 30 (2018) e1802405.
- [44] S.H. Shin, Y.E. Bae, H.K. Moon, J. Kim, S.H. Choi, Y. Kim, H.J. Yoon, M.H. Lee, J. Nah, *ACS Nano*, 11 (2017) 6131-6138.
- [45] L. Shi, R. Yang, S. Lu, K. Jia, C. Xiao, T. Lu, T. Wang, W. Wei, H. Tan, S. Ding, *NPG Asia Materials*, 10 (2018) 821-826.